초기값을 갖는 비동질무한영역의 해석을 위한 비례경계무한요소법

Infinite Element for the Scaled Boundary Analysis of Initial Valued on-Homogeneous Elastic Half Space

이 계 희† Andrew J. Deeks*
Lee, Gye-Hee
(논문접수일 : 2008년 3월 25일 ; 심사종료일 : 2008년 4월 20일)

요 지

본 논문에서는 초기값을 갖는 비동질 반무한 평면문제를 비례경계유한요소법으로 해석하기 위하여 무한요소를 이 해석법에 도입하였다. 초기값을 갖는 반무한 평면의 자유면은 비례경계좌표계의 원주방향의 좌표를 이용하여 모델링하였고 무한요소는 이 자유면이 나타내는 무한한 영역을 모사하기 위해 사용되었다. 반무한 평면의 물성치(탄성계수)에 대한 초기값은 비례중심의 위치와 비례경계좌표계에서의 반지름 멱함수를 이용하여 나타내었다. 사상형 무한요소를 사용하여 일관된 정식화가 가능하였고, 제안된 해석법에 대한 적용성과 성능을 두 수치예제를 통하여 보였다.

핵심용어 : 비례경계 해석, 무한 비동질 반무한 평면, 사상형 무한요소

Abstract

In this paper, to analyze the initial valued non-homogeneous elastic half space by the scaled boundary analysis, the infinite element approach was introduced. The free surface of the initial valued non-homogeneous elastic half space was modeled as a circumferential direction of boundary scaled boundary coordinate. The infinite element was used to represent the infinite length of the free surface. The initial value of material property(elastic modulus) was considered by the combination of the position of the scaling center and the power function of the radial direction. By use of the mapping type infinite element, the consistent elements formulation could be available. The performance and the feasibility of proposed approach are examined by two numerical examples.

Keywords *: scaled boundary analysis, initial valued non-homogeneous half space, mapping type infinite element*

1. Introduction

The infinite domain, such as ground, is one of head-ache problems to engineers. To solve this problem, various approaches were proposed and are proposing. Especialy, the coupling of two conventional analysis method, such as, the finite element approaches with infinite elements(Lui etc., 2003; Yang etc., 2003; Lui etc., 2003), the finite element approaches with the boundary element approaches(Kim etc., 2002; Spyrakos etc., 2003) and even the meshless methods with infinite elements(Gu etc., 2001; Kireev etc., 2006), were introduced for the coupling of a finite domain and a infinite domain.

Recently, the approach called scaled boundary finite method(Wolf, 2002)(SBFEM) was proposed, and based on its semi-analytic properties, the infinite fields, such as ground in the geo-technical area (Doherty etc., 2003; Hassanen etc.,2007), and the analytic field, such as crack tip(Yang etc., 2006;),

† 책임저자, 정회원 · 목포해양대학교 해양시스템공학부 부교수
Tel: 061-240-7314 : Fax: 061-240-7301
E-mail: lghlsk@mmu.ac.kr
* Professor, University of Western Australia

• 이 논문에 대한 토론을 2008년 6월 30일까지 본 학회에 보내주시면 2008년 8월호에 그 결과를 게재하겠습니다.

were successfully simulated by this method. In this approach, bounded(finite) domains and unbounded (infinite) domains are treated as the same manners.

To represent the engineering properties of deep soil layer, the non-homogeneous elastic half space is normally used. The scaled boundary finite element method was already extended to this problem(Doherty etc., 2003;Lee, 2007). In these studies, the soil layer was modeled as unbounded domain and its scaling center should be strictly located on free surface to represent the variation of soil property following power function of depth. This location of scaling center at the free surface made it possible to take the advantage of side face modeling, but the free surface should have the zero stiffness. The improved approach of this study was proposed(Doherty etc., 2005), but its zero elastic modulus at surface was not overcome. Generally, in real engineering problem, the surface of ground has nonzero initial value of elastic modulus. Our study started to apply the nonzero initial elastic modulus to the previous study. Furthermore, in most of engineering field, the plane problem is more feasible than axisymmetric problem, especially, one dimensionally long structures, such as strip footing, rail way, trench structure and so on. To satisfy this demand, new equations of scaled boundary finite element method for plane problems are needed.

In our study, the infinite element is introduced to scaled boundary method to represent the initial valued half space, and the equations of scaled boundary finite element method for non-homogeneous plane are derived by a virtual work scheme(Deeks etc., 2002). Two numerical examples are provided for the verification and the demonstration of practical application.

2. Initial valued non-homogeneous elasticity

To consider the initial valued non-homogeneous half space, it is assumed the unbounded domain with the elevated scaling center at(0, y_1).(Figure 1) In this model, the horizontal surface is modeled by circumferential direction differed from that the infinite edges

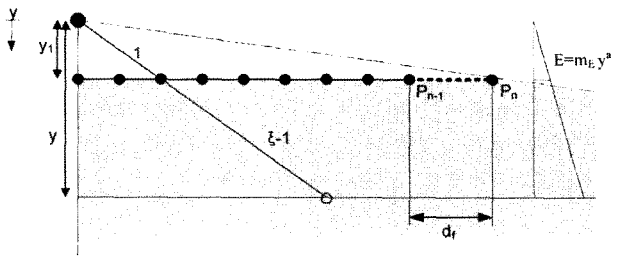

Figure 1 Half space model by unbounded domain had elevated scaling center

are normally modeled by side faces in the scaled boundary manner. Therefore, the free surface should be discretized.

If elastic modulus can be assumed as follows,(Doherty etc., 2003)

$$E = m_E y^{\alpha} \tag{1}$$

where m_E is a constant and α is the parameter of non-homogeneous. The elastic modulus of surface can be determined by two variable y_1 and α.

$$E_0 = m_E y_1^{\alpha} \tag{2}$$

The elastic modulus as scaled boundary coordinate can be obtained as follows

$$E(\xi, s) = m_E(\xi y(s))^{\alpha} = m_E \xi^{\alpha}(y(s))^{\alpha} \tag{3}$$

For a line passing discretized boundary, the elastic modulus in depth y can be obtained as follows

$$\frac{1}{\xi} = \frac{y_1}{y} \tag{4}$$

$$y(s) = y_1 = \frac{y}{\xi} \tag{5}$$

$$E = m_E \xi^{\alpha}\left(\frac{y}{\xi}\right)^{\alpha} = m_E y^{\alpha} \tag{6}$$

By the Eq(6), the elastic modulus of depth y is the function of y, but it is independent from ξ. Therefore, the initial valued non-homogeneous half space can be modeled by this approach. However, the following points should be considered.

- For a bounded domain, this method is not valid, because, the gap y_1 in Figure 1 is hard to be

configured in a bounded domain.

- If $d_f \to \infty$, this model can represent a half space, otherwise, this model is not a real half space. But it can be used as a approximation.

In most engineering problems, the material properties of near field modeled by bounded domain are unvaried for the engineering purpose.(footings, back fill material and so on) Furthermore, the combined use of another computational methods, such as finite element method, can sufficiently analyze the complex behaviors of the near field without considerations of infinite domain(Doherty etc., 2005; Ekevid etc., 2006). Therefore, the first point can't be a defect of this approach. The second point is able to be solved by introducing of infinite element to the last boundary element. This is the main topic of this study.

3. Scaled boundary Infinite Element method

3.1 Mapping type infinite element

The main feature of the scaled boundary method is the semi-analytic approach. The radial direction is assumed in analytic manner, and the circumferential direction is discretized. The derivation of the basic equation was already performed by several approaches. (Wolf, 2002; Deeks etc., 2002; Doherty etc., 2003) In this study, the notation of(Doherty etc., 2003) will be used.

If the axisymmetric case is assumed, the scaling center should be located on the axis of symmetry. In plane strain or stress problems, the scaling center can be located horizontally anywhere. The vertical location of the scaling center can be determined as the initial value of elastic modulus and the non-homogeneous parameter. But it should be over the free surface.

The discretized boundary S is represented by a set of points($r_s(s)$, $z_s(s)$), where s is the boundary co-ordinate measuring the distance around S from a selected origin to the point. In the infinite element approach, the unbounded domain assumption is essential, so the domain is described by $1 \le \xi < \infty$.

In elastic-static problem, the strain ε can be denoted as

$$\varepsilon = \mathbf{L} \cdot \mathbf{u} \tag{7}$$

where, $\mathbf{L}$ is the linear differential operator and $\mathbf{u}$ is the displacement field of domain, respectively. In the scaled boundary approximation of axisymmetric problem, Eq.(7) can be rewritten as follows.

$$\{\varepsilon_h(\xi,s)\} = \begin{bmatrix} \frac{\partial}{\partial r} & 0 \\ 0 & \frac{\partial}{\partial z} \\ \frac{1}{r} & 0 \\ \frac{\partial}{\partial z} & \frac{\partial}{\partial r} \end{bmatrix} \{u_h(\xi,\eta)\} \tag{8}$$

where, $\{\varepsilon_h(\xi,s)\}$ is the approximated strain field, $\{u_h(\xi,s)\}$ is the approximated displacement field, $r = \xi r_s(s)$, $z = \xi z_s(s)$ are the horizontal and vertical coordinate denoted in the scaled boundary transformation. For the plane strain or stress problem, the third row of Eq.(8) is ignored.

To represent the infinite length of element, the coordinates can be represented by the infinite mapping function $[M]$.

$$s = [M(\eta)]\{s_i\} \tag{9}$$

where, $[M(\eta)]$ is the infinite mapping function, $\{s_i\}$ is the nodal s coordinates at the circumferential boundary. Since, the straight line is permitted only in the infinite mapping,

$$r_s(s) = s\cos(\theta) \tag{10a}$$

$$z_s(s) = s\sin(\theta) \tag{10b}$$

where, θ is the angle between s coordinate and Cartesian coordinate. The infinite mapping function is used only in the mapping of geometry. In the interpolation of displacement, another functions(shape functions) are used. The infinite mapping function of linear, quadratic and cubic are listed in Table

Table 1 Infinite mapping functions

node	linear		quadratic		cubic	
	M_i	$\partial M_i/\partial\eta$	M_i	$\partial M_i/\partial\eta$	M_i	$\partial M_i/\partial\eta$
i	$\frac{2}{(1-\eta)}$	$\frac{2}{(1-\eta)^2}$	$\frac{-2\eta}{(1-\eta)}$	$\frac{-2}{(1-\eta)^2}$	$\frac{(-1+9\eta^2)}{4(1-\eta)}$	$\frac{(-1+18\eta-9\eta^2)}{4(1-\eta)^2}$
j	-	-	$\frac{(1+\eta)}{(1-\eta)}$	$\frac{2}{(1-\eta)^2}$	$\frac{(4-8\eta-12\eta^2)}{4(1-\eta)}$	$\frac{(-4-24\eta+12\eta^2)}{4(1-\eta)^2}$
k	-	-	-	-	$\frac{(1+4\eta+3\eta^2)}{4(1-\eta)}$	$\frac{(5+6\eta-3\eta^2)}{4(1-\eta)^2}$
l	-	-	-	-	-	-

1(Bettess, 1992).

As following the procedure represented in(Doherty etc., 2003), the relationship between the axisymmetric coordinate and the scaled boundary coordinate is follows,

$$\begin{Bmatrix} \frac{\partial}{\partial r} \\ \frac{\partial}{\partial z} \end{Bmatrix} = \frac{1}{|J|}\begin{bmatrix} z_{s,s}(s) & -z_s(s) \\ -r_{s,s}(s) & r_s(s) \end{bmatrix}\begin{Bmatrix} \frac{\partial}{\partial \xi} \\ \frac{1}{\xi}\frac{\partial}{\partial s} \end{Bmatrix} \tag{11}$$

where,

$$|J| = \left|r_s(s)z_{s,s}(s) - z_s(s)r_{s,s}(s)\right| \tag{12}$$

$$r_s(s)_{,s} = \cos(\theta) \tag{13}$$

$$z_s(s)_{,s} = \sin(\theta) \tag{14}$$

Therefore, the linear differential operator **L** can be denoted as follows.

$$\mathbf{L} = [b^1(s)]\frac{\partial}{\partial\xi} + [b^2(s)]\frac{1}{\xi}\frac{\partial}{\partial s} + [b^3(s)]\frac{1}{\xi} \tag{15}$$

where,

$$\begin{aligned} [b^1(s)] &= \frac{1}{|J|}\left[[L^1]z_s(s)_{,s} - [L^2]r_s(s)_{,s}\right] \\ [b^2(s)] &= \frac{1}{|J|}\left[-[L^1]z_s(s) + [L^2]r_s(s)\right] \\ [b^3(s)] &= [L^3]\frac{1}{r_s(s)} \end{aligned} \tag{16}$$

$$[L^1] = \begin{bmatrix} 1 & 0 \\ 0 & 0 \\ 0 & 0 \\ 0 & 1 \end{bmatrix},\quad [L^2] = \begin{bmatrix} 0 & 0 \\ 0 & 1 \\ 0 & 0 \\ 1 & 0 \end{bmatrix},\quad [L^3] = \begin{bmatrix} 0 & 0 \\ 0 & 0 \\ 1 & 0 \\ 0 & 0 \end{bmatrix} \tag{17}$$

In the plane strain or stress problems, the third rows of $[L^1]$,$[L^2]$ are ignored and $[L^3]$ become zero matrix. To obtain coefficient matrix, the following matrix are assumed.

$$\begin{aligned} [B^1(s)] &= [b^1(s)][N(s)] \\ [B^2(s)] &= [b^2(s)][N(s)]_{,s} + [b^3(s)][N(s)] \end{aligned} \tag{18}$$

where, $[N(s)]$ is the shape function to be used the interpolation of the nodal displacements. $[N(s)]_{,s}$ can be denoted as follows

$$\frac{dN(s)}{ds} = \frac{dN(\eta)}{d(\eta)}\frac{d\eta}{ds} \tag{19}$$

If the quadratic mapping function is assumed(Table 1), the s can be denoted as follows

$$\begin{aligned} s &= [M_i(\eta)M_j(\eta)]\{s_i s_j\}^T \\ &= M_i(\eta)s_i + M_j(\eta)s_j \end{aligned} \tag{20}$$

The derivative of s is

$$ds = (M_i(\eta)_{,\eta}s_i + M_j(\eta)_{,\eta}s_j)d\eta \tag{21}$$

Therefore, $\frac{d\eta}{ds}$ is denoted

$$\frac{d\eta}{ds} = \frac{2(s_j - s_i)}{(1-\eta)^2} \tag{22}$$

The shape function $[N(s)]$ is different from $[M(\eta)]$. So, the infinite element for SBFEM is not an isoparametric element.

3.2 Derivation for non-homogeneous plane problems

The derivation of scaled boundary equations for axisymmetric problems is presented in(Doherty etc., 2003). The equations for the plane strain or stress problems are newly derived here.

The approximate stress of domain is

$$\{\sigma_h(\xi,s)\}=[D(s)]\xi^{\alpha}\{\varepsilon_h(\xi)\}$$
$$=[D(s)]\xi^{\alpha}\{[B^1(s)]\{u_h(\xi)\}_{,\xi}+\frac{1}{\xi}[B^2(s)]\{u_h(\xi)\}\} \quad (23)$$

The corresponding virtual strain is

$$\{\delta\varepsilon(\xi,s)\}=\{[B^1(s)]\{u(\xi)\}_{,\xi}+\frac{1}{\xi}[B^2(s)]\{u_h(\xi)\}\} \quad (24)$$

The bounded case($0\le\xi\le1$) is assumed and the side-face load and the body force are ignored firstly. In this condition, the virtual work statement becomes

$$\int_V\{\delta\varepsilon(\xi,s)\}^T\{\sigma_h(\xi,s)\}dV-\int_S\{\delta u(s)\}^T\{t(s)\}ds=0 \quad (25)$$

where $dV=|J|\xi d\xi ds$ and $|J|$ is the Jacobian of the boundary elements. In Eq.(25), the first term represents the internal work and the second term is the external work.

Substituting the Eq.(23) and(24) into Eq.(25), the internal work term is

$$\int_V\{\delta\varepsilon(\xi,s)\}^T\{\sigma_h(\xi,s)\}dV$$
$$=\int_s\int_0^1\{[B^1(s)]\{u_h(\xi,s)\}_{,\xi}+\frac{1}{\xi}[B^2(s)]\{u_h(\xi,s)\}\}^T$$
$$\times[D(s)]\xi^{\alpha}\{[B^1(s)]\{u_h(\xi,s)\}_{,\xi}+\frac{1}{\xi}[B^2(s)]\{u_h(\xi,s)\}\}\xi d\xi ds$$
$$=\int_0^1\{\delta u(\xi)\}_{,\xi}^T\left[\xi^{\alpha+1}[E^0]\{u_h(\xi)\}_{,\xi}+\xi^{\alpha}[E^1]^T\{u_h(\xi)\}\right]d\xi$$
$$+\int_0^1\{\delta u(\xi)\}^T\left[\xi^{\alpha}[E^1]\{u_h(\xi)\}_{,\xi}+\xi^{\alpha-1}[E^2]\{u_h(\xi)\}\right]d\xi \quad (26)$$

where the coefficient matrices of Eq.(26) are defined

$$[E^0]=\int_s[B^1(s)]^T D(s)[B^1(s)]|J|ds \quad (27)$$

$$[E^1]=\int_s[B^2(s)]^T D(s)[B^1(s)]|J|ds \quad (28)$$

$$[E^2]=\int_s[B^2(s)]^T D(s)[B^2(s)]|J|ds \quad (29)$$

The integrals containing the term $\{\delta u(\xi)\}_{,\xi}^T$ in Eq.(26) are integrated with respect ξ using Green's Theorem

$$\int_0^1\{\delta u(\xi)\}_{,\xi}^T\left[\xi^{\alpha+1}[E^0]\{u_h(\xi)\}_{,\xi}+\xi^{\alpha}[E^1]^T\{u_h(\xi)\}\right]d\xi$$
$$=\{\delta u\}^T\left[[E^0]\{u_h\}_{,\xi}+[E^1]^T\{u_h\}\right]$$
$$-\int_0^1\{\delta u(\xi)\}^T\left[\xi^{\alpha+1}[E^0]\{u_h(\xi)\}_{,\xi\xi}+(\alpha+1)\xi^{\alpha}[E^0]\{u_h(\xi)\}_{,\xi}\right]d\xi$$
$$-\int_0^1\{\delta u(\xi)\}^T\left[\xi^{\alpha}[E^1]^T\{u_h(\xi)\}_{,\xi}+\alpha\xi^{\alpha-1}[E^1]^T\{u_h(\xi)\}\right]d\xi \quad (30)$$

The external work term in Eq.(25) is expressed as follows(Deeks etc., 2002)

$$\int_s\{\delta u(s)\}^T\{t(s)\}ds=\{\delta u\}^T\int_s\{N(s)\}^T\{t(s)\}ds \quad (31)$$

The integral of right hand side in Eq.(31) can be denoted as the equivalent nodal forces $\{P\}$ due to the boundary traction. Combining Eqs(26),(30) and(31), the virtual work statement in Eq(25) becomes

$$\{\delta u\}^T\left[[E^0]\{u_h\}_{,\xi}+[E^1]^T\{u_h\}\right]-\{\delta u\}^T\{P\}$$
$$+\int_0^1\{\delta u(\xi)\}^T\left[-\xi^{\alpha+1}[E^0]\{u_h(\xi)\}_{,\xi\xi}-(\alpha+1)\xi^{\alpha}[E^0]-\{u_h(\xi)\}_{,\xi}\right.$$
$$-\xi^{\alpha}[E^1]^T\{u_h(\xi)\}_{,\xi}-\alpha\xi^{\alpha-1}[E^1]^T\{u_h(\xi)\}+\xi^{\alpha}[E^1]\{u_h(\xi)\}_{,\xi}$$
$$\left.+\xi^{\alpha-1}[E^2]\{u_h(\xi)\}\right]d\xi=0 \quad (32)$$

To satisfy for all $\{\delta u(\xi)\}^T$, both of the following condition must be satisfied.

$$\{P\}=\left[[E^0]\{u_h\}_{,\xi}+[E^1]^T\{u_h\}\right] \quad (33)$$

$$\xi^{\alpha+1}[E^0]\{u_h(\xi)\}_{,\xi\xi}$$
$$+[(\alpha+1)[E^0]+[E^1]^T-[E^1]]\xi^{\alpha}\{u_h(\xi)\}_{,\xi}+[\alpha[E^1]^T-[E^2]]\xi^{\alpha-1}=0 \quad (34)$$

If a vector $\{F_t(\xi)\}$ denotes the variation of side face load in ξ direction, the external virtual work done by the tractions on side face is

$$\int_0^1 \{\delta u(\xi)\}^T \{F_t(\xi)\} d\xi \tag{35}$$

Including Eq.(35) in the Eq.(32) and multiplying ξ in both sides of Eq.(34), the final displacement equation of non-homogeneous space for plane strain and stress problems becomes

$$\xi^{\alpha+2}[E^0]\{u_h(\xi)\}_{,\xi\xi} + \xi^{\alpha+1}[(\alpha+1)[E^0]+[E^1]^T-[E^1]]\{u_h(\xi)\}_{,\xi} + \xi^{\alpha}[\alpha[E^1]^T-[E^2]]+\xi\{F_t(\xi)\}=0 \tag{36}$$

4. Solution procedures

The general solution of Eq.(36) can be obtained by solving of homogeneous equation, ignoring the side face load($\{F_t(\xi)=0\}$). The general solution is the linear combination of the independent nodal displacement modes $\{\phi_i\}$ of boundary such that

$$\{u_h(\xi)\} = c_1\xi^{-\lambda_1}\{\phi_1\} + c_2\xi^{-\lambda_2}\{\phi_2\} + \cdots \tag{37}$$

where c_i are the integration coefficient that represents the contribution of each displacement mode to the entire solution. And λ_i determines the profile of the nodal displacement modes in radial direction.

The displacements for each mode take the form

$$\{u_h(\xi)\} = \xi^{-\lambda_i}\{\phi_i\} \tag{38}$$

Substituting Eq.(38) to the homogeneous form of Eq.(36) yields the following

$$\left[\lambda_i^2[E^0]+\lambda_i([E^1]-[E^1]^T-\alpha[E^0])+(\alpha[E^1]^T-[E^2]\right]\{\phi_i\} \tag{39}$$

The equivalent nodal forces $\{q\}$ need to equilibrate each nodal displacement mode is as following(Deeks etc., 2002)

$$\{q_i\} = [[E^1]^T - \lambda_i[E^0]]\{\phi_i\} \tag{40}$$

The quadratic eigen problem can be converted to linear eigen problem by rearranging Eq.(40) and substituting to Eq.(39). However the size of linear eigen problem is doubled. The rearranged Eq.(40) is

$$\lambda_i\{\phi_i\} = [E^0]^{-1}\left[[E^1]^T\{\phi_i\} - \{q_i\}\right] \tag{41}$$

Substituting Eq.(41) to Eq.(39) and solve for $\lambda_i\{q_i\}$, following equation is obtained

$$\lambda_i\{q_i\} = \left[[E^1][E^0]^{-1}[E^1]^T - [E^2]\right]\{\phi_i\} + \left[\alpha[I]-[E^1][E^0]^{-1}\right]\{q_i\} \tag{42}$$

Gathering the Eq.(41) and (42) in form of eigen problem and omitting the subscripts, the linear eigen problem expression of Eq.(39)

$$\begin{bmatrix} [E^0]^{-1}[E^1]^T & -[E^0]^{-1} \\ [E^1][E^0]^{-1}[E^1]^T - [E^2] & \alpha[I]-[E^1][E^0]^{-1} \end{bmatrix} \begin{Bmatrix}\phi\\ q\end{Bmatrix} = \lambda \begin{Bmatrix}\phi\\ q\end{Bmatrix} \tag{43}$$

This expression of axisymmetric problems is represented in(Doherty etc., 2003)

$$\begin{bmatrix} [E^0]^{-1}[E^1]^T & -[E^0]^{-1} \\ [E^1][E^0]^{-1}[E^1]^T & (\alpha+1)[I]-[E^1][E^0]^{-1} \end{bmatrix} \begin{Bmatrix}\phi\\ q\end{Bmatrix} = \lambda \begin{Bmatrix}\phi\\ q\end{Bmatrix} \tag{44}$$

To get the particular solution corresponding to the side face loading, the side face loading is assumed as the power function of ξ

$$\{F_t(\xi)\} = \xi^t\{F_t\} \tag{45}$$

The particular solution of Eq.(36) is as following (Doherty etc., 2003)

$$\{u_t(\xi)\} = \xi^{t-\alpha+1}\{\phi_t\} \tag{46}$$

Substituting Eq.(46) into Eq.(36) yields

$$\left[(t^2+(2-\alpha)t+1-\alpha)[E^0]+(\alpha-1-t)[E^1]+(1+t)[E^1]^T - [E^2]\right]\xi^{t+1}\{\phi_t\} + \xi^{t+1}\{F_t\} = 0 \tag{47}$$

Therefore the displacement modes corresponding to side face loading is

$$\{\phi_t\} = \Big[(t+1)(t-\alpha+1)[E^0] - (t-\alpha+1)[E^1] + (t+1)[E^1]^T - [E^2]\Big]^{-1}\{-F_t\} \tag{48}$$

The side face loading displacement modes for axisymmetric problem(Doherty etc., 2003) is

$$\{\phi_t\} = \Big[(t-\alpha)(t-\alpha+1)[E^0] + (t-\alpha+1)[(\alpha+2)[E^0] + [E^1]^T - [E^1]] + (\alpha+1)[E^1]^T - [E^2]\Big]^{-1}\{-F_t\} \tag{49}$$

The complete displacement solution including side face loadings and boundary loadings are represented as

$$\{u_h(\xi,s)\} = [N(s)]\left(\xi^{t-\alpha+1}\{\phi_t\} + \sum_{i=1}^{n} c_i \xi^{-\lambda_i}\{\phi_i\}\right) \tag{50}$$

The corresponding stress of domain is

$$\{\sigma_h(\xi,s)\} = [D(s)]\xi^t[(t-\alpha+1)[B^1(s)] + [B^2(s)]]\{\phi_t\} + [D(s)]\sum_{i=1}^{n} c_i \xi^{\alpha-\lambda_i-1}[-\lambda_i[B^1(s)] + [B^2(s)]]\{\phi_i\} \tag{51}$$

The detail equations omitted in this paper is same as the standard scaled boundary finite element approach (Wolf,2002; Deeks etc., 2002).

5. Examples

5.1 Embedded strip foundation

A stiff strip type footing, embedded in a non-homogeneous half plane, was analyzed to show the performance of infinite element approach. Several types of load were applied on the surface of the footing.(Fig. 2) In this example, the elastic modules of footing $E_f = 2000$ was assumed, and modulus for ground $m_E = 100$ and $\alpha = 0.5$ were used. Poisson ratio of each domain was 0.3 and plane strain behavior was assumed.

Firstly, a prescribed horizontal displacement load was applied on the surface of footing. The vertical displacement of this analysis is shown Fig. 3. In this

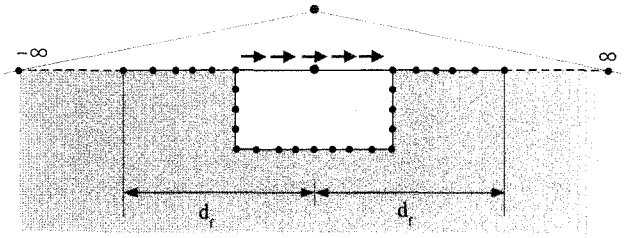

(a) Infinite approach

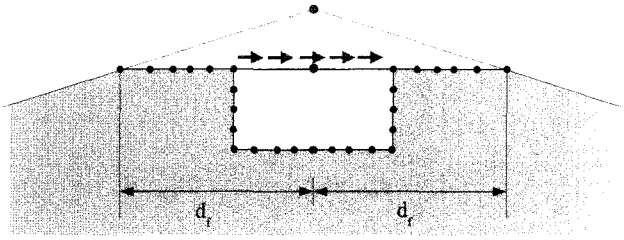

(b) Approximation approach

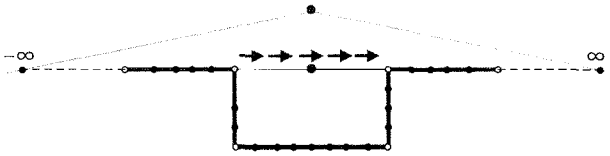

(c) Edge definition

Figure 2 Embedding strip footing

figure, the vertical displacements and the rotation angle of footing show different behavior as modeling type. In case of infinite approach, the vertical displacements and the rotation angle are denoted consistent trend, while those of the approximation approach are remarkable changed as analysis range d_f. The behaviors of approximated model are converged to those of infinite approach as increasing of analysis range.

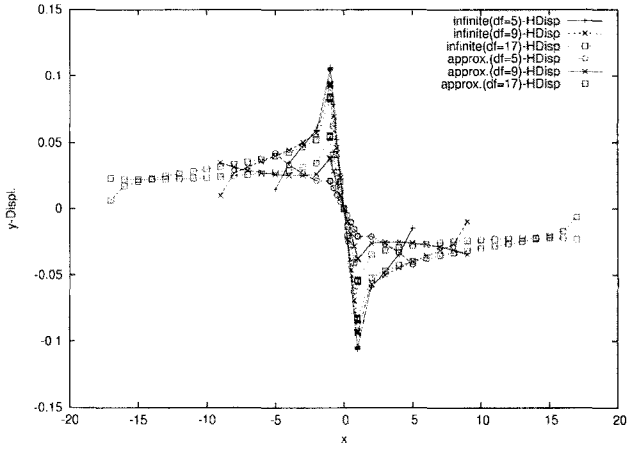

Figure 3 Vertical displacements due to horizontal displacement

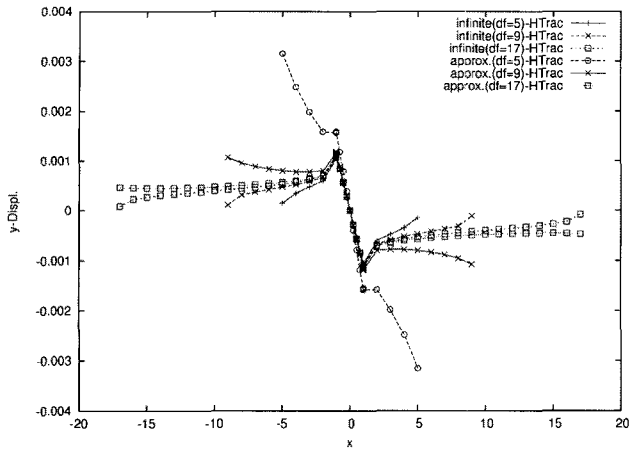

Figure 4 Vertical displacements due to horizontal traction

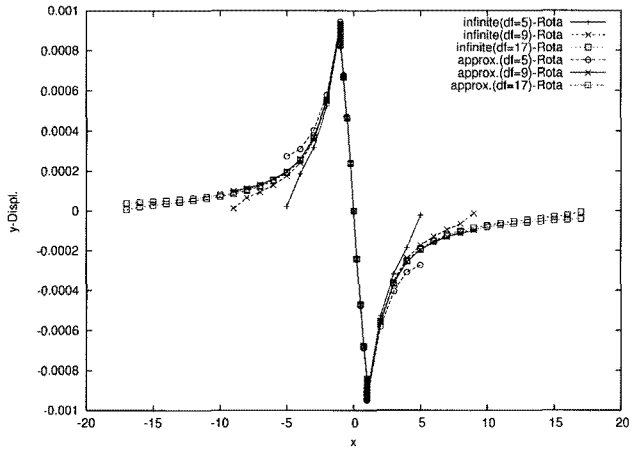

Figure 5 Vertical displacements due to rotational load

The vertical displacements of nodes due to horizontal traction on the surface of footing were also estimated.(Fig. 4) In these figure, the different between two approach are more severe. The responses of infinite model show the consistent manner again, but the responses of approximated one show the big divergences as analysis range. In these traction load case, the relative magnitude of approximated and infinite displacements is reversed.

The behaviors of half plane including stiff footing due to rotational load are shown in Fig. 5. Different from previous examples, there are little different between the infinite approach and the approximated approach. This means that the truncation effects of approximated model are remarkable in case of asymmetry. The half model and axisymmetric model are hard to represent these types of differences.

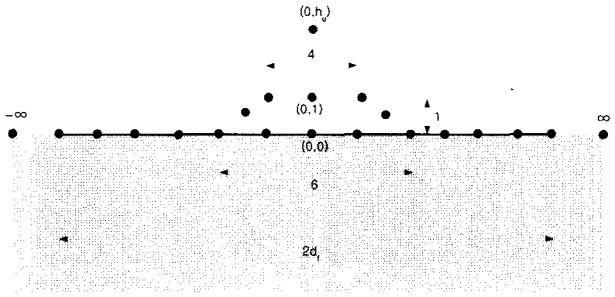

Figure 6 Foundation on half space

5.2 Surface strip foundation

A strip footing on non-homogeneous half space was analyzed. A stiff trapezoid shape footing on soft ground was assumed. The elastic modulus of footing was $E_f = 10000$. Because, homogeneous material for footing was assumed, $\alpha_f = 0$. The scaling center of this bounded domain was located the center of footing top surface.

The ground supporting the footing was assumed non-homogeneous half space and its material modulus was assumed $m_E = 100$. The value of non-homogeneous parameter was changed to several values and, its effects were observed. This ground was modeled unbounded domain and its scaling center was located at $(0,h)$. This location could be changed to represent the adequate elastic modulus of ground surface.

To show the effects of infinite region, the comparison of stress profile beneath the footing was made. In Fig. 7, the shear stress profile of approximated analysis came closer as the analysis radius d_f increasing. This shows the efficient of infinite element approach. Each analysis used the same element size, so the total degrees of freedom of infinite analysis are same as the smallest case of approximated approaches.

The effects of non-homogeneous parameter are show in Fig. 8. In this analysis, the elastic modulus of each model were identical(=125), so the locations of the scaling centers were determined as α by Eq.(2). In this figure, as increasing the values of α, high stress areas are moved to nearby of footing. This means that the failure of ground would be occurred near of the footing in case of high α value.

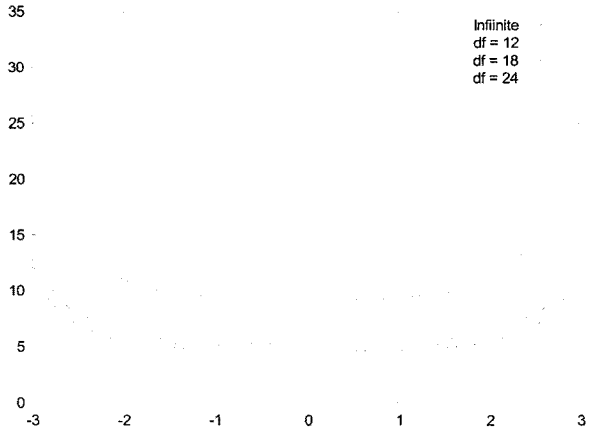

Figure 7 Stress profiles beneath the footing

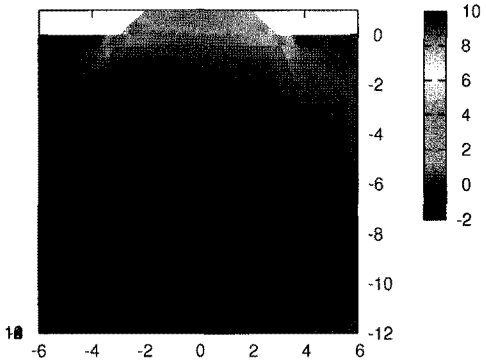

(a) $\alpha = 0.1$

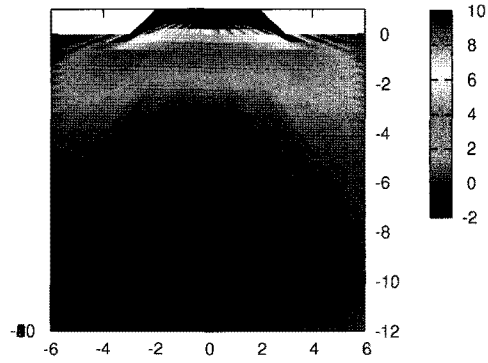

(b) $\alpha = 0.5$

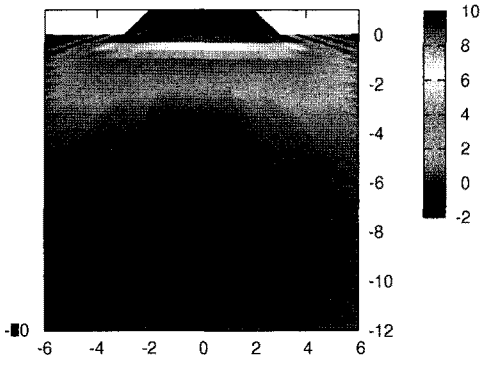

(c) $\alpha = 0.9$

Figure 8 Stress contour as α values

6. Conclusion

To represent the initial valued non-homogeneous half space by SBFEM, infinite element approaches were adopted to circumferential direction of this method. By this modification and additional derivation of non-homogeneous domain for the half plane, the feasibility of scaled boundary method can be more expanded to real engineering problems.

The advantages of this approach compared to normal approximation by truncation are remarkable in lateral direction loading in both displacement and stress field. The effects of the non-homogeneous parameter α are appeared by stress concentration at beneath of the footing.

Acknowledgements

This work was supported by the Korea Research Foundation Grant funded by the Korean Government. (MOEHRD, Basic Research Promotion Fund)(KRF-2007-D00475).

References

Bettess, P. (1992) *Infinite Elements*, First edition, Penshaw Press.

Deeks, A.J., Wolf, J.P. (2002) A virtual work derivation of the scaled boundary finite element method for elastostatic, *Computational Mechanics*, 28, pp.489~504.

Doherty, J.P., Deeks, A.J. (2003), Scaled finite element analysis of a non-homogeneous elastic half space, *Int. J. for numerical methods in engineering*, 57, pp.955~973.

Doherty, J.P., Deeks, A.J. (2005) Adaptive coupling of the finite-element and scaled boundary finite-element methods for non-linear analysis of unbounded medi, *Computer & Geotechnics*, 32, pp.436~444.

Ekevid, T., Lane, H., Wiberg, N.E. (2006) Adaptive solid wave propagation influences of boundary conditions in high-speed train applications, *Computational Methods in applied Mechanics and Engineering*, 195, pp.236~250.

Gu, Y.T., Liu, G.R. (2001) A coupled element free Galerkin boundary element method for stress analysis of two dimensional solids, *Computational Methods in applied Mechanics and Engineering*, 190, pp.4405~4419.

Hassanen, M., El-Hamalawi, A. (2007) Two-dimensional development of the dynamic coupled consolidation scaled boundary finite-element method for fully saturated soils, *Soil Dynamics & Earthquake Engineering*, 27, pp.153~165.

Kim, M.K., Lim, Y.M., Cho S.Y., Choa, K.H., Lee, K.W. (2002) Seismic analysis of base-isolated liquid storage tanks using the BE-FE-BE coupling technique, *Soil Dynamics and Earthquake Engineering*, 22, pp.1151~1158.

Kireev, O., Mertens, T., Bouillard, Ph. (2006) A coupled EFGM-CIE method for acoustic radiation, *Computers and Structures*, 84, pp.2092~2099.

Lee, G.H. (2007) Scaled boundary finite element methods for non-homogeneous half plane, *J. of computational structural engineering institute of Korea*, 20(2), pp.127~136(in Korean).

Liu, D.S., Chiou, D.Y., Lin, C.H. (2003) 3D IEM formulation with an IEM/FEM coupling scheme for solving elastostatic problems, *Advances in Engineering Software*, 34, pp.309~320.

Liu, D.S., Chiou D.Y., Lin, C.H. (2004) A hybrid 3D thermo-elastic in nite element modeling for area-array package solder joints, *Finite Elements in Analysis and Design*, 40, pp.1703~1727.

Spyrakos, C.C., Xu, C. (2003) Seismic soil-structure interaction of massive flexible strip-foundations embedded in layered soils by hybrid BEM-FEM, *Soil Dynamics and Earthquake Engineering*, 23, pp.383~389.

Wolf, John P. (2003) The scaled boundary finite element method, *John Wiley & Sons*.

Yang, Y.B., Hung, H.H., Chang, D.W. (2003) Train-induced wave propagation in layered soils using finite/infinite element simulation, *Soil Dynamics and Earthquake Engineering*, 23, pp.263~278.

Yang, Z. (2006) Fully automatic modelling of mixed-mode crack propagation using scaled boundary finite element method, *Engineering Fracture Mechanics*, 73, pp.1711~1731.